

# Seismic Response Analysis of Steel Structure Isolation System Under Long-Period Seismic Motion

Long Yu<sup>1\*</sup>, Mei Sheng<sup>1</sup>, Huan Feng<sup>1</sup>, Jianan Hu<sup>2</sup>

<sup>1</sup>Chuzhou Polytechnic, Chuzhou 239000, Anhui Province, China

<sup>2</sup>Hefei Urban Construction Development Co., Ltd., Hefei 230031, Anhui Province, China

\*Corresponding author: Long Yu, yulong@chzc.edu.cn

**Copyright:** © 2024 Author(s). This is an open-access article distributed under the terms of the Creative Commons Attribution License (CC BY 4.0), permitting distribution and reproduction in any medium, provided the original work is cited.

**Abstract:** To analyze the seismic response of steel structure isolation systems under long-period seismic motion, a 9-story steel frame building was selected as the subject. Five steel structure finite element models were established using SAP2000. Response spectrum analysis was conducted on the seismic motion to determine if it adhered to the characteristics of long-period seismic motion. Modal analysis of each structural model revealed that the isolation structure significantly prolonged the structural natural vibration period and enhanced seismic performance. Base reactions and floor displacements of various structures notably increased under long-period seismic motion compared to regular seismic activity. Placing isolation bearings in the lower part of the structure proved more effective under long-period seismic motion. In seismic design engineering, it is essential to consider the impact of long-period seismic motion on structures and the potential failure of isolation bearings.

**Keywords:** Long-period seismic motion; Steel structure; Mid-story isolation structure; Isolation bearing; Seismic performance

**Online publication:** June 18, 2024

## 1. Introduction

The advancement of our country's "dual-carbon" goals has provided new opportunities and challenges for the development of steel structures for green buildings<sup>[1,2]</sup>. Research on steel structures has progressed from seismic-resistant structures to seismic isolation and mitigation structures. New theoretical research on steel structures, such as dual seismic-resistant systems and double-layer isolation systems, has emerged in domestic and international studies<sup>[3-5]</sup>. However, there is limited literature on the seismic performance of steel structures under long-period seismic motion. Long-period seismic motion typically lasts from several seconds to over ten seconds<sup>[6-10]</sup> and exhibits distinctive low-frequency characteristics, often associated with relatively modest peak accelerations. In particular geological and soil conditions, there may be an amplification effect on seismic amplitudes<sup>[6,11]</sup>.

Research on structural seismic performance under long-period seismic motion mainly focuses on concrete structures, with no literature found on the seismic performance of steel structure isolation systems. This paper establishes various models of steel structures under multiple working conditions. By comparing the seismic response

values of each structure under long-period seismic motion, the influence of long-period seismic motion on structural seismic performance is analyzed. Factors considered in setting isolation bearings under long-period seismic motion are discussed, providing a reference for the practical application of steel structure isolation systems in engineering.

## 2. Engineering overview and establishment of structural models

### 2.1. Engineering overview

The project described in this paper is a 9-story vertically irregular steel structure building, with a bottom podium floor height of 4.5 m and a total height of 9 m. The main structure has a floor height of 3.3 m. The seismic design intensity for the structure is 7 degrees, with a seismic acceleration of 0.10 g. The site category is Type II, and the design earthquake group is the first group, classified as a Class C building. The finite element model of the steel structure is shown in **Figure 1**. The dimensions of the steel structure columns and braces are listed in **Table 1**, where box columns are filled with C30 concrete. The dimensions of the steel structure beams are provided in **Table 2**. The reinforced concrete structure floor has a thickness of 100 mm, the walls are constructed using 200 mm autoclaved aerated concrete blocks.

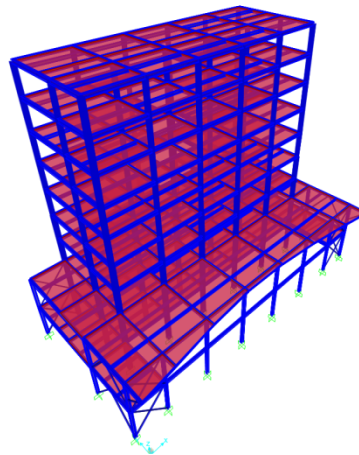


**Figure 1.** 3D Model of the steel structure

**Table 1.** Steel structure column and support size

No.	Size/mm	Steel grade	Note
GZ1	500×18	Q345B	Box steel column
GZ2	500×16	Q345B	Box steel column
GZ3	450×16	Q345B	Box steel column
GZ4	400×16	Q345B	Box steel column
GZ5	300×300×12×16	Q345B	H steel column
GC	159×5	Q235B	Circular steel pipe brace

**Table 2.** Steel structure beam size

No.	Size/mm	Steel grade	Note
GL1	400×250×10×16	Q345B	Welded I-beam
GL2	350×250×10×14	Q345B	Welded I-beam
GL3	300×200×10×12	Q345B	Welded I-beam

## 2.2. Structural model establishment

In order to analyze the influence of long-period seismic motion on the seismic performance of the steel structure isolation system, we established the original structural model of the steel structure and the base-isolated structural model. Additionally, to analyze the effect of different locations for the placement of isolation bearings on the seismic performance of the steel structure, we created isolation bearing models with bearings placed on the third, fifth, and seventh floors.

We used SAP2000 to establish the aforementioned five models, and the finite element model of the original structure is shown in **Figure 1**. We defined the beam, column, and brace properties of the steel structure using frame section properties, and the reinforced concrete floor slabs were defined using shell elements with section properties. The dead load and live load of the floor were both applied in the form of distributed loads on the floor, and the self-weight load of the interior and exterior infill walls was applied as distributed line loads on the upper flange of the beams. In the structural modeling process, the floor nodes were specified using node constraints with diaphragm constraints to ensure that the floor stiffness was set to infinite rigidity.

## 2.3. Selection of seismic isolation bearings

To meet the requirements for the support area and minimum diameter of the isolation bearings, while considering the matching of the bearing diameter with the structural column size, rubber isolation bearings LNR400 are installed at the base of the columns around the podium. Lead-rubber bearings LRB400 were installed at the base of the corner and edge columns of the main structure, and LRB500 was installed at the base of the middle columns on the ground floor of the main structure. The number and type of isolation bearings installed on the upper part of the main structure were consistent with those on the ground floor of the main structure, all set at the base of the structural layer columns. The isolation bearing was defined using the connecting property rubber isolator unit and the isolation bearings were drawn using two-point connection elements with a spacing of 0.8 meters. For the lead-rubber bearings, the connection properties U2 and U3 components were set as nonlinear connections. The selected isolation-bearing parameter information is shown in **Table 3**.

**Table 3.** Performance parameters of isolation bearing

Model	Effective diameter (mm)	Total thickness of rubber (mm)	Pre-yield stiffness (kN/m)	Horizontal equivalent stiffness (kN/m)	Vertical stiffness (kN/mm)	Yield force (kN)
LNR400	400	73	—	660	1600	—
LRB400	400	73	8790	820	2200	27
LRB500	500	92	10910	1010	2400	40

## 3. Seismic motion selection and characteristic analysis

### 3.1. Seismic motion selection

There is currently no standardized definition for long-period seismic motion. The long-period seismic motion was selected based on Wang *et al.*, Zhang *et al.*, and Fang *et al.*'s works <sup>[9,10,12]</sup>, and three long-period seismic motions and regular seismic motions were selected from the PEER database and Lu *et al.*'s work <sup>[13]</sup>. The selected parameters are described in **Table 4**.

**Table 4.** Selected earthquake seismic motion information

Seismic motion type	Earthquake location, station (date, magnitude)	Seismic motion name	Pga/(cm/s <sup>2</sup> )	Duration (s)	Abbreviation in this paper
Ordinary Seismic Motion	Imperial Valley, El Centro (1940, <i>M</i> 6.5)	El Centro NS	341.7	30	El
	Kern County, Taft Lincoln School (1952, <i>M</i> 7.3)	KERN AF021	155.8	54.35	TAF021
	San Fernando, Buena Vista-Taft (1971, <i>M</i> 6.6)	SFERN BVP090	11.9	26.65	BVP090
Long-period Seismic Motion	Kern County, LA-Hollywood Stor FF (1952, <i>M</i> 7.3)	KERN.PEL PEL090	41.4	70	PEL090
	Chi-Chi Taiwan, China, CHY092 (1999, <i>M</i> 7.6)	CHICHI CHY092 N	82.7	150	CHY092
	Kahramanmaraş Turkey, 3123 (2023, <i>M</i> 7.8)	Turkey 3123 NS	651.9	125	Turkey

### 3.2. Seismic response spectrum analysis

Figure 2 shows the seismic acceleration response spectrum. It can be seen from the figure that the response spectrum of ordinary earthquake motions was relatively concentrated, exhibiting peak accelerations within a short period of time. In contrast, the response spectrum of long-period seismic motions not only had peaks in the early stage but also exhibited double peaks or even multiple peaks within the structural resonance period, showing significant differences compared to ordinary earthquake motions.

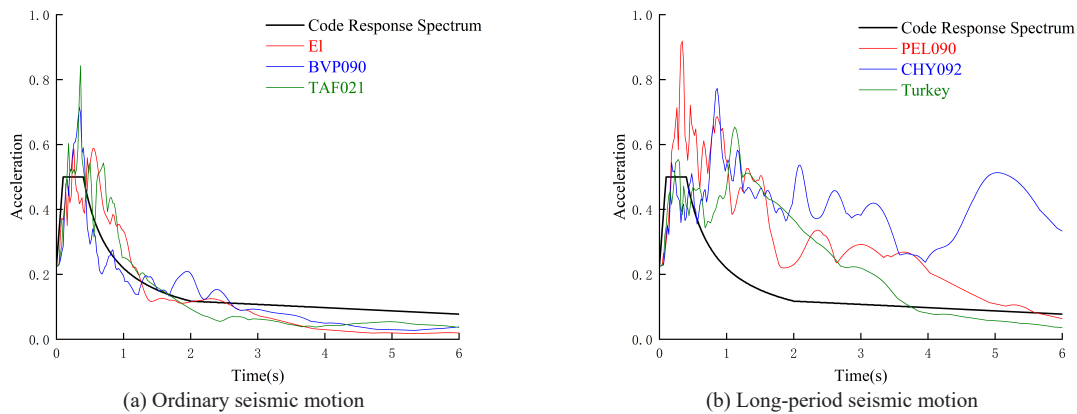


**Figure 2.** Seismic motion acceleration response spectrum

## 4. Modal analysis of structure

Through modal analysis of various steel structure models, the first six natural vibration periods of the structure were obtained (Table 5). By comparing the data of the original structure and the seismic isolation structure, it can be seen that the natural vibration periods of the seismic isolation structure have significantly increased compared to the original structure. In the first mode of translational motion, the natural vibration period of the base-isolated structure increased by 93.4% compared to the original structure, while the three-story isolated structure increased by 95.3%. Comparing the natural vibration periods of three-story, five-story, and seven-story isolated structures, it is observed that the natural vibration period gradually decreases, but still shows a significant extension compared to the original structure. In the second mode of translational motion and the third mode of torsional motion, the natural vibration periods of the isolated structures increased to varying degrees compared to the original structure. Additionally, the natural vibration period gradually decreased as the seismic isolation bearings were placed at different floor levels above the third floor. This indicates that seismic isolation bearings can prolong the natural vibration period of the structure, enhance structural ductility,

and improve seismic performance. Among the first three natural vibration periods, the structure exhibited the longest natural vibration period when the seismic isolation bearings were placed on the third floor.

**Table 5.** Natural vibration period of structure (s)

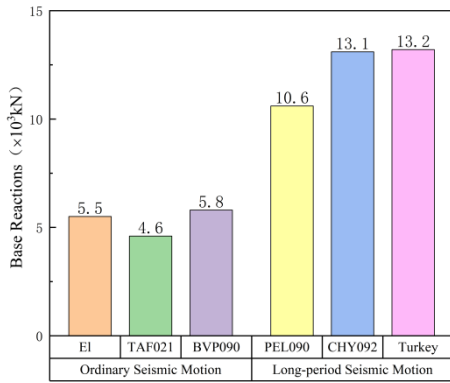
Mode	Original structure	Base isolation at the foundation level	Three-story base isolation	Five-story base isolation	Seven-story base isolation
1	1.629	3.159	3.181	2.741	2.191
2	1.624	3.147	3.151	2.726	2.178
3	1.253	2.357	2.759	2.352	1.844
4	0.578	0.952	0.696	0.700	0.937
5	0.568	0.915	0.665	0.647	0.906
6	0.450	0.855	0.577	0.490	0.705

## 5. Long-period earthquake seismic motion response analysis

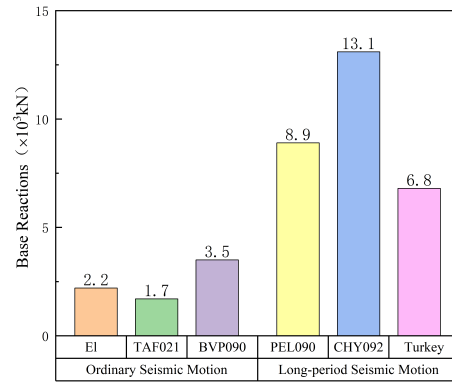
### 5.1. Base shear force

When analyzing the rare earthquake effects on various models, the input peak ground acceleration of the seismic motion was adjusted proportionally to  $220 \text{ cm/s}^2$  [14]. FNA was used for the analysis. The numerical values of the base reaction forces are shown in **Figure 3**. In the original structure, under the long-period seismic motion in Turkey, the base reaction force increased by 127.6% compared to the ordinary seismic motion BVP090. Under the long-period seismic motion, the average base reaction force increased by 132.1% compared to the average value of the ordinary seismic motion. In the base-isolated structure, under the long-period seismic motion CHY092, the base reaction force increased by 274.3% compared to the ordinary seismic motion BVP090. Under the long-period seismic motion, the average base reaction force increased by 289.2% compared to the average value of the ordinary seismic motion. As for the three-story, five-story, and seven-story base-isolated structures in inter-story isolation, under the long-period seismic motion, the maximum base reaction force increased by 78.3%, 67.2%, and 129.4% respectively compared to the maximum value of the ordinary seismic motion. Under the long-period seismic motion, the average base reaction force increased by 67.3%, 57.9%, and 96.6% respectively compared to the average value of the ordinary seismic motion.

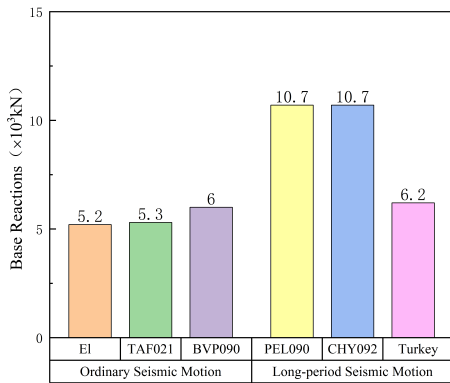
From the comparative data, it can be seen that the base reaction forces of the structures under long-period seismic motion increased significantly compared to ordinary seismic motion, with the greatest impact on the base-isolated structures. In inter-story isolation, as the elevation of the isolation support positions increased, the difference between the maximum base reaction force under long-period seismic motion and ordinary seismic motion tended to increase. However, the difference between the average base reaction force under long-period seismic motion and ordinary seismic motion was the smallest in the five-story base-isolated structure.



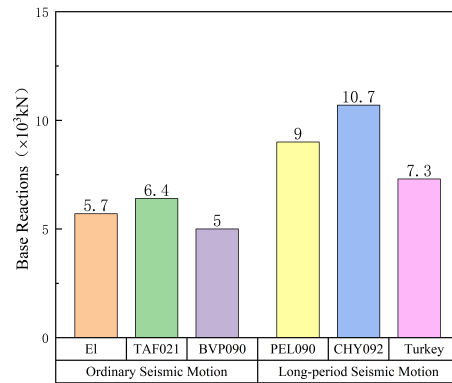
(a) Original structure



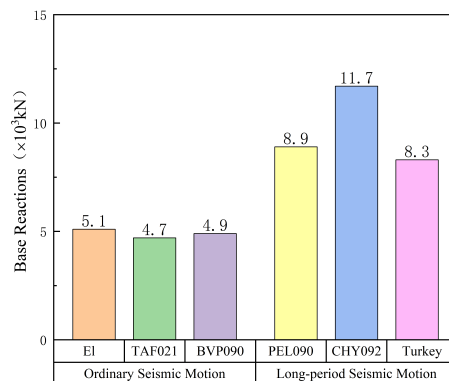
(b) Base isolation at the foundation level



(c) Three-story base isolation



(d) Five-story base isolation



(e) Seven-story base isolation

**Figure 3.** Structural base reaction force

## 5.2. Floor displacement

**Figure 4** shows floor displacements. In the original structure, the floor displacements under long-period seismic motion increased significantly compared to ordinary seismic motion, indicating a significant difference in structural seismic response between long-period and ordinary seismic motions. In base-isolated structures, the floor displacements under long-period seismic motion also showed a substantial increase compared to ordinary seismic motion. Additionally, there were differences in floor displacements between different types of long-period seismic motions, highlighting the notable impact of long-period seismic motion on base-isolated structures. A comparison of three-story, five-story, and seven-story base-isolated structures reveals that as the elevation of isolation support positions increased, the floor displacements gradually decreased, demonstrating the influence of isolation support position on structural seismic performance.

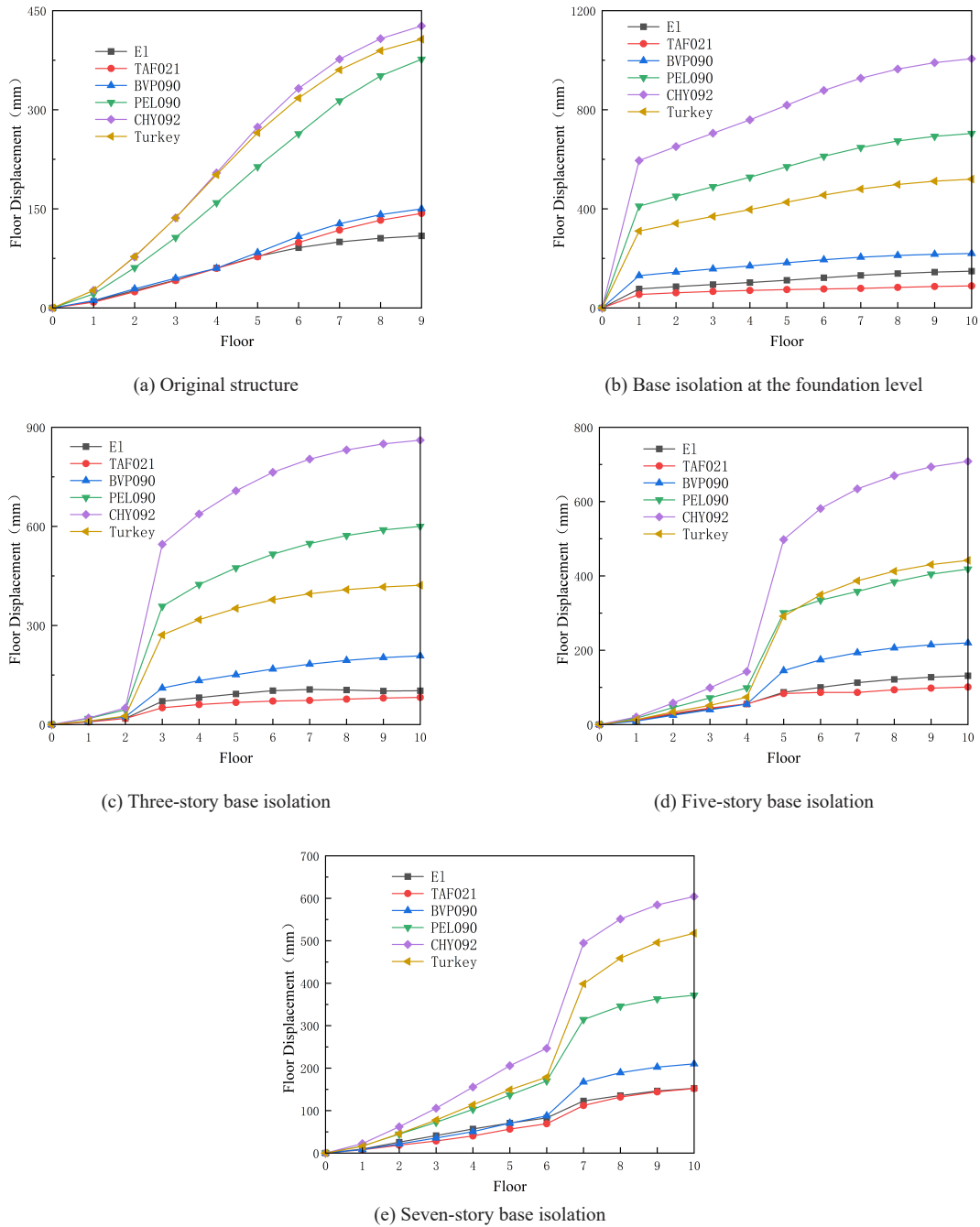


Figure 4. Floor displacement

### 5.3. Displacement of isolation layers

The limit horizontal displacement of the base isolation bearing under compressive stress should be greater than the maximum value between 0.55 times the effective diameter of the isolation bearing and 3 times the total thickness of rubber inside the bearing <sup>[14]</sup>. Under the premise of meeting safety requirements, the limit horizontal displacement of the base isolation bearing was set at 220 mm. According to the data in **Table 6**, the displacements of the isolation layer under ordinary seismic action were all less than the horizontal displacement limit of the base isolation bearing. Under the action of long-period seismic motion, both the base-isolated structure and the three-story base-isolated structure have isolation layer displacements greater than the horizontal displacement limit of the base isolation bearing, indicating that the isolation bearings no longer meet the displacement requirements.

Under the CHY092 seismic motion, the isolation layer displacements of the five-story base-isolated structure and the seven-story base-isolated structure exceed the limit horizontal displacement of the base isolation bearing, indicating differences in structural response to different long-period seismic motions.

**Table 6.** Displacement of isolation layer (mm)

Seismic motion type	Seismic motion abbreviation	Base isolation at the foundation level	Three-story base isolation	Five-story base isolation	Seven-story base isolation
Ordinary seismic motion	EI	76.8	52.1	31.7	40.1
	TAF021	54.3	32.8	27.6	42.9
	BVP090	130.5	87.3	90.1	79.6
Long-period seismic motion	PEL090	410.9	<u>313.4</u>	202.0	144.6
	CHY092	594.9	495.6	355.5	<u>248.1</u>
	Turkey	310.5	<u>245.5</u>	217.9	219.7

Note: The underlined values in the table are all greater than the limit horizontal displacement of the isolation support.

## 6. Conclusion

- (1) Through response spectrum analysis of seismic motion, the selected seismic motion was further examined for characteristics such as frequency spectrum to determine whether it is a long-period seismic motion. Modal analysis was conducted on various steel structure models, revealing a significant increase in the natural vibration period of the base-isolated structures compared to the original structures. The placement of base isolation bearings effectively reduces the impact of earthquakes on the structures. As the elevation of the base isolation bearing positions increases, there is a decreasing trend in the natural vibration period of the base-isolated structures, indicating that the positioning of base isolation bearings influences the natural vibration period of the structures.
- (2) A comparative analysis of the seismic responses of various structures to long-period seismic motion and ordinary seismic motion shows that under long-period seismic motion, the base shear forces of various structures significantly increase compared to ordinary seismic motion. The floor displacements of various structures also experience significant increases, indicating that long-period seismic motion is detrimental to the seismic resistance of steel structures. The elevation of the base isolation bearings affects the seismic performance of the structures, with the ideal scenario being the placement of base isolation bearings at lower levels within the structures.
- (3) Analysis of the base isolation bearings reveals that under the action of long-period seismic motion, the displacements of the base isolation bearings in the base-isolated structures and three-story base-isolated structures exceed the limits. In seismic design of engineering structures, the influence of long-period seismic motion should be fully considered, while also taking into account the impact of the positioning of base isolation bearings on the seismic performance of the structures.

## Funding

- (1) Anhui Province Young and Middle-aged Teacher Training Action Excellent Young Teacher Cultivation Project (YQYB2023162)
- (2) Anhui University Natural Science Research Key Project (KJ2021A1410)



(3) Special Topic of the Higher Education Institution Scientific Research Development Center of the Ministry of Education (ZJXF2022080)

## Disclosure statement

The authors declare no conflict of interest.

## References

- [1] Shen Z, Luo J, Li Y, 2016, Discussion on Coordinated Development of Urbanization, Industrialization, and Informatization with Steel Buildings as Objects in the Construction Industry. *Progress in Steel Building Structures*, 18(02): 1–6 + 25.
- [2] Bao S, 2023, Urgent Need to Achieve Deep Integration of the Steel-Steel Structure-Building Industry Chain. *China Metallurgical News*, October 24, 2023.
- [3] Wang L, Tan J, Wang M, 2023, Conception of Structural Seismic Design Based on Double Carbon Goals. *Steel Construction (Chinese & English)*, 38 (10): 32–41.
- [4] Millichamp D, Tirca L, 2022, Dual System for Enhanced Seismic Performance of Friction-Sliding Braced Frames. Springer International Publishing, 641–649.
- [5] Sipan Y, Rais A, 2016, Evaluation of Seismic Performance Factors in High Rise Steel Buildings with Dual Lateral Systems Consisting of Buckling Restrained Braced Frames and Intermediate Moment Frames. *Procedia Engineering*, 161: 680–686.
- [6] Dai M, 2020, Quantitative Identification and Simulation of Far-Field Long-Period Seismic Motions, dissertation, Chongqing University.
- [7] Sun Z, Li X, Li H, et al., 2023, Analysis on the Seismic Response of RC Bridge Piers Under Long-Duration Earthquake Seismic Motions. *Journal of Basic Science and Engineering*, 31(01): 154–169.
- [8] Heidarpour A, Zhao X, Hayashi K, et al., 2023, Seismic Performance of Concrete-Filled Steel Tube Columns Using Ultra-High-Strength Steel Under Long-Period Seismic Motion Demands. *Advances in Structural Engineering*, 26(12): 2160–2171.
- [9] Wang B, Zhang J, Zheng R, et al., 2023, Seismic Response Analysis of Air-Cooled Supporting Structure Under Long-Period Seismic Motion. *Earthquake Engineering and Engineering Dynamics*, 43(04): 104–117.
- [10] Zhang L, Xia T, 2023, Study on the Overturning Resistance of Base-Isolated Structure under the Action of Long-Period Seismic Motion. *Journal of Natural Disasters*, 32(04): 170–180.
- [11] Zhou W, Liu D, Zhao J, et al., 2023, Seismic Response Analysis of Mid-Story Isolation High-Rise Building Structure under Three-Dimensional Long Period Seismic Motion. *Journal of Nanjing Tech University (Natural Science Edition)*, 45(02): 188–195.
- [12] Fang X, Fan C, Miao M, 2023, Seismic Fragility Analysis of Water Tower Under Long-Period Seismic Motions. *Guangdong Architecture Civil Engineering*, 30(07): 63–67.
- [13] Lu X, Qin S, Xu Z, 2023, Enlightenment of Turkey M7.8 Earthquake on China's Earthquake Prevention and Disaster Reduction. *Cities and Disaster Reduction*, 2023(02): 1–8.
- [14] Ministry of Housing and Urban-Rural Development of the People's Republic of China, Code for Seismic Design of Buildings, GB 50011-2010 (2016 Edition).

### Publisher's note

Bio-Byword Scientific Publishing remains neutral with regard to jurisdictional claims in published maps and institutional affiliations.